JOURNAL OF VIROLOGY, Apr. 2004, p. 3502–3513 Vol. 78, No. 7
0022-538X/04/$08.00+0 DOI: 10.1128/JVI.78.7.3502–3513.2004

High-Throughput Screening of the Yeast Kinome: Identification of Human Serine/Threonine Protein Kinases That Phosphorylate the Hepatitis C Virus NS5A Protein

Carlos Coito,[1] Deborah L. Diamond,[1] Petra Neddermann,[2] Marcus J. Korth,[1] and Michael G. Katze[1,3]*

Department of Microbiology[1] and Washington National Primate Research Center,[3] University of Washington, Seattle, Washington 98195, and IRBM Merck, Rome, Italy[2]

Received 7 October 2003/Accepted 4 December 2003

The hepatitis C virus NS5A protein plays a critical role in virus replication, conferring interferon resistance to the virus through perturbation of multiple intracellular signaling pathways. Since NS5A is a phosphoprotein, it is of considerable interest to understand the role of phosphorylation in NS5A function. In this report, we investigated the phosphorylation of NS5A by taking advantage of 119 glutathione *S*-transferase-tagged protein kinases purified from *Saccharomyces cerevisiae* to perform a global screening of yeast kinases capable of phosphorylating NS5A in vitro. A database BLAST search was subsequently performed by using the sequences of the yeast kinases that phosphorylated NS5A in order to identify human kinases with the highest sequence homologies. Subsequent in vitro kinase assays and phosphopeptide mapping studies confirmed that several of the homologous human protein kinases were capable of phosphorylating NS5A. In vivo phosphopeptide mapping revealed phosphopeptides common to those generated in vitro by AKT, p70S6K, MEK1, and MKK6, suggesting that these kinases may phosphorylate NS5A in mammalian cells. Significantly, rapamycin, an inhibitor commonly used to investigate the mTOR/p70S6K pathway, reduced the in vivo phosphorylation of specific NS5A phosphopeptides, strongly suggesting that p70S6 kinase and potentially related members of this group phosphorylate NS5A inside the cell. Curiously, certain of these kinases also play a major role in mRNA translation and antiapoptotic pathways, some of which are already known to be regulated by NS5A. The findings presented here demonstrate the use of high-throughput screening of the yeast kinome to facilitate the major task of identifying human NS5A protein kinases for further characterization of phosphorylation events in vivo. Our results suggest that this novel approach may be generally applicable to the screening of other protein biochemical activities by mechanistic class.

Phosphorylation is a common posttranslational processing event in the synthesis of proteins, and changes in the degree of protein phosphorylation play an important role in modulating protein function. Many cellular processes, including signal transduction, transcription, protein synthesis, and cell growth and differentiation, are regulated by phosphorylation-dependent mechanisms (17, 19). Therefore, it is not surprising that the protein kinases, a family of enzymes that catalyze the phosphorylation of proteins, comprise one of the largest families of genes in eukaryotes. The protein kinase complement of the human genome (the human "kinome") is estimated to comprise about 1.7% of all human genes, with a total of 518 genes identified according to a cataloging approach published recently (19). The presence of such a large number of kinases in the human genome represents a significant challenge to protein kinase studies, suggesting that it would be extremely powerful to develop high-throughput approaches for characterizing kinase-substrate reactions. Although a recent study describes the use of a microarray format for the high-throughput analysis of substrate specificity of yeast protein kinases (36), the use of such an approach to identify the human kinase(s) responsible for phosphorylation of a biological substrate has not been previously described.

There has been much interest in characterizing the role of protein phosphorylation in mechanisms associated with viral infection, pathogenesis, and persistence (16, 35). In this regard, it is well established that the hepatitis C virus (HCV) nonstructural 5A (NS5A) protein is a phosphoprotein and that phosphorylation of NS5A is highly conserved among HCV genotypes and other members of the *Flaviviridae* family (13, 23, 25). This led to the idea that phosphorylation may play a role in the flavivirus life cycle and inspired our interest in obtaining a better understanding of NS5A phosphorylation, particularly since this protein has been implicated in resistance of HCV to interferon treatment (4, 5, 27). NS5A is phosphorylated primarily on serine residues both in vitro and in vivo (13, 15, 22, 23, 25, 30). Although the effects of various kinase inhibitors have implicated a cellular serine/threonine kinase(s) from the CMGC kinase group (25), it should be noted that this group contains several kinase families, and these studies did not identify a particular kinase in the phosphorylation of NS5A. More recent in vitro kinase assays specifically demonstrated that NS5A can be phosphorylated by casein kinase 2 (CK2) (12, 14) and protein kinase A (PKA) (12).

The interferon-induced double-stranded RNA-activated protein kinase, PKR, is a key component of the antiviral and antiproliferative effects induced by interferon. NS5A forms a

* Corresponding author. Mailing address: Department of Microbiology, University of Washington, Box 358070, Seattle, WA 98195-8070. Phone: (206) 732-6135. Fax: (206) 732-6056. E-mail: honey@u.washington.edu.

complex with PKR, disrupting PKR dimerization, which results in repression of PKR function and inhibition of PKR-mediated eIF-2α phosphorylation. Whether NS5A is a substrate of PKR is yet to be determined. There is no PKR homologue in the yeast kinome, but the yeast kinase GCN2 still has sequence homology with PKR. In this study, we were particularly interested in finding out whether GCN2 is a kinase of NS5A.

In this report, we further investigated the phosphorylation of NS5A using a kinome-scale high-throughput screening approach in order to identify human protein kinases that phosphorylate NS5A. The approach is based on a biochemical genomics strategy, originally described by Martzen et al. (20), for constructing an array of molecular constructs for expression of all yeast kinases (the yeast kinome) (11, 19). Our long-term interests are to gain insight into the role of phosphorylation in the ability of NS5A to modulate a multitude of cellular signaling pathways. Although there are already more than 518 known human kinases, more than four times the number of the kinases in yeast, we reasoned that the yeast kinome would represent a good model for beginning a global inspection of NS5A phosphorylation activity, since phosphorylation of NS5A occurs primarily at serine residues (13, 15, 22, 23, 25, 30) and the major families of serine/threonine kinases are conserved between yeast and humans. The use of the yeast model was based on the idea that the kinase(s) phosphorylating NS5A is very likely to be evolutionarily conserved. This is supported by our previous findings that Ser 2194 is a major phosphorylation site among all HCV genotypes and this site can be phosphorylated by yeast, insect, and mammalian kinases (13). We screened 119 glutathione S-transferase (GST)-tagged protein kinases purified from *Saccharomyces cerevisiae* in a global effort to identify yeast kinases capable of phosphorylating NS5A in vitro. BLAST searches were performed to identify the closest human sequence homologs, and commercially available sources of human protein kinases were used for subsequent in vitro NS5A kinase assays. We demonstrated that several of these human kinases were capable of phosphorylating NS5A in vitro, some of which play a major role in protein translation and antiapoptotic pathways that are regulated by NS5A. Furthermore, the phosphopeptide pattern of NS5A isolated from COS-1 cells suggests that the phosphorylation sites used in vivo were similar to those observed in vitro, allowing us to identify kinases of particular interest for further characterization of NS5A phosphorylation. Finally, rapamycin studies revealed that p70S6 kinase and potentially closely related family members phosphorylate NS5A inside the cell.

MATERIALS AND METHODS

Reagents. The human kinases AKT1, MEK1, MKK6, MKK7β1, SGK1, p70S6K, CHK2, PDK1, and the rat kinases CK1 delta and p90S6K were purchased from Upstate Biotechnology (Lake Placid, N.Y.). The purity and activity of these kinases were certified by the manufacturer but were not independently verified in this study. All materials used for GST-yeast kinase purification were obtained from Amersham Biosciences Corp. (Piscataway, N.Y.). Radiolabeled ATP, [γ-^{32}P]ATP, and [^{32}P]orthophosphoric acid in water were purchased from NEN Life Science Products, Inc. (Boston, Mass.). Dulbecco's modified eagle medium (DME), phosphate-free DME, Hanks' balanced salt solution, and calf serum were purchased from Gibco/Invitrogen Corp. (Grand Island, N.Y.). The *S. cerevisiae* protein kinases (119 constructs), cloned in the plasmid pYEX4T-1 and expressed in the EJ758 yeast strain (36), were provided by Eric M. Phizicky (University of Rochester, Rochester, N.Y.).

Purification of GST-yeast kinases. Colonies representing transformants of the EJ758 yeast strain were obtained on plates containing synthetic minimal (SD) minus Ura media. These colonies were then used to inoculate SD minus Ura liquid medium and grown for 8 h. At this time, each inoculum was split 1 to 10 into SD minus Ura minus Leu medium and grown for an additional 16 h. When the cultures reached an optical density at 600 nm of 0.8, the cells were induced with 0.5 mM $CuSO_4$ for 2 to 3 h prior to harvesting by centrifugation at 4°C for 5 min at 1,500 × *g*. After induction, the cells were washed twice in two to four pellet volumes of ice-cold water. The washed cell pellet was resuspended in 1 ml of homogenization buffer (50 mM Tris-HCl [pH 7.5], 1 mM EDTA, 4 mM $MgCl_2$, 1 mM dithiothreitol [DTT], 10% glycerol, 250 mM NaCl) containing 1× protease inhibitor mix, and extracts were made with glass beads (15 pulses, 30 s each at 4°C) using a multichannel vortexer. Extracts were transferred to 15-ml conical tubes and centrifuged at 4°C for 5 min at 450 × *g*. The supernatants were then centrifuged at 4°C for 30 min at 10,000 × *g*. The GST-kinases were purified from the resulting supernatants by glutathione-agarose chromatography (20). Briefly, the supernatants were incubated with prewashed reduced glutathione-agarose beads for 1 h at 4°C and then extensively washed in the same buffer (50 mM Tris-HCl [pH 7.5], 500 mM NaCl, 10% glycerol, 4 mM $MgCl_2$). Aliquots of 33% slurries (150 μl each) were flash frozen in an ethanol-dry ice bath and stored at −80°C for later use.

In vitro yeast kinase assay. Baculovirus recombinant NS5A (2 μl, 100 ng), purified from Sf9 cells as previously described (13), was added to 50 μl of purified GST-kinase bound to glutathione-agarose beads prepared as described above. The final amount of kinase added was normalized based on the relative recovery of each purified kinase as determined by Western blotting with an antibody to GST. The phosphorylation reaction was carried out at 30°C for 60 min in a final volume of 60 μl containing yeast kinase buffer (50 mM Tris-HCl [pH 7.2], 10 mM $MgCl_2$, 1 mM DTT) supplemented with protease and phosphatase inhibitors and a mixture of [γ-^{32}P]ATP and ATP with a predetermined specific activity (~5,000 dpm/pmol of ATP), such that the reaction mixture contained at least a 1,000-fold excess of ATP over the NS5A protein concentration. Human recombinant casein kinase 2 (hCK2) was used as a positive control to demonstrate NS5A phosphorylation. Glutathione-agarose beads, incubated with the yeast EJ758 strain expressing an empty glutathione vector, were used as a negative control to demonstrate that phosphorylation of NS5A resulted from the appropriate GST-kinase and not from the nonspecific binding of other proteins to either GST or the beads. The kinase reaction was terminated by flash freezing the samples in an ethanol-dry ice bath. An equal volume of 2× SDS protein loading buffer (125 mM Tris-HCl [pH 6.8], 20% glycerol, 2% SDS, 2% β-mercaptoethanol, 0.02% bromophenol blue) was added, and the samples were boiled at 95 to 100°C for 5 min prior to analysis by SDS-polyacrylamide gel electrophoresis (PAGE) (10% gel). After resolving the samples, the gel was dried using a slab gel dryer SGD 4050 (Savant) for 5 h at 80°C and then exposed to X-ray film at −70°C with an intensifying screen.

In vitro human kinase assay. The phosphorylation reaction was carried out in the presence or absence of 100 ng of baculovirus recombinant NS5A (purified from Sf9 cells) in a final volume of 40 μl of human kinase buffer (20 mM morpholinepropanesulfonic acid [pH 7.2], 25 mM β-glycerol phosphate, 5 mM EGTA, 1 mM sodium orthovanadate, 1 mM DTT, 10 mM $MgCl_2$) containing a mixture of [γ-^{32}P]ATP and ATP with a predetermined specific activity (~5,000 dpm/pmol of ATP) such that the reaction mixture contained at least a 1,000-fold excess of ATP over the NS5A protein concentration. The appropriate kinase was added and assayed for phosphorylation of NS5A. The buffer condition used was that recommended by the enzyme supplier. The kinases assayed, and the amount used per reaction, were 20 mU of rat casein kinase 1 (rCK1 delta), 0.5 μg of hAKT1, 0.5 U of hMEK1, 0.05 μg of hMKK6, 0.2 μg of hMKK7β1, 0.025 μg of hSGK1, 10 mU of hp70S6K, 20 mU of rp90S6K, 10 ng of hPDK1, 100 mU of hCHK2, or 0.05 μg of hCK2. For samples containing rCK1 delta, hAKT1, hSGK1, hCHK2, hp70S6K, or hCK2 (positive control), the reaction was allowed to proceed for 10 min at 30°C. For samples containing hPDK1, rp90S6K, hMEK1, hMKK6, hMKK7β1, or hCK2 (positive control), the reaction was allowed to proceed for 30 min at 30°C.

Two-dimensional phosphopeptide mapping. For two-dimensional phosphopeptide mapping, the phosphorylated samples were resolved by SDS–10% PAGE and then transferred to a nitrocellulose membrane. Radiolabeled phosphoproteins were detected by autoradiography. The ^{32}P-containing bands were excised, kept wet in water, and incubated in 0.5% polyvinylpyrrolidone–100 mM acetic acid for 1 h at 37°C in order to block nonspecific adsorption of proteases. Control slices were prepared from the same-molecular-weight region of lanes corresponding to phosphorylation reactions containing kinase only or NS5A only. The slices were then washed thoroughly with deionized water (five times, 1 ml per wash) followed by 50 mM ammonium bicarbonate, pH 8.3 (five times, 1

ml per wash), and finally resuspended in 80 μl of 50 mM ammonium bicarbonate, pH 8.3. Proteolytic digestion was accomplished by adding 1 μg of trypsin and incubating for 3 h at 37°C, followed by another 1-μg addition and incubation at 37°C overnight. The next day, a third addition of 1 μg of trypsin was made, and the samples were incubated for 2 h at 37°C prior to adding 1 μg of chymotrypsin and digesting for 3 h at 37°C. A second addition of 1 μg of chymotrypsin was made, and the samples were incubated at 37°C for 3 h or overnight. The supernatants containing soluble peptides were then transferred to a separate tube, and the slices were washed with 400 μl of water to extract any remaining peptides. The pooled supernatant and wash were dried with a speed vac, and the peptides were subsequently suspended in 10 μl of buffer (7.8% acetic acid, 2.2% formic acid). Phosphopeptide recovery was monitored at every step by Cerenkov counting. The resuspended samples were loaded onto cellulose thin-layer chromatography (TLC) plates (20 cm by 10 cm) and electrophoresed in the first dimension (20 cm) at 1,000 V for 60 min in reverse polarity (positive to negative). After the plates were dried overnight in the fume hood, separation in the second dimension was achieved by ascending chromatography in 37.5% *n*-butanol, 25% pyridine, and 7.5% acetic acid. The plates were dried extensively, and radiolabeled phosphopeptides were detected by autoradiography.

In vivo [^{32}P]orthophosphoric acid labeling. COS-1 cells (0.5×10^6) were cultured in a T-25 flask for 15 h prior to transfection with 10 μg of a pcDNA3 construct encoding the NS5A-1b protein. Transfections were performed using the SuperFect kit (Qiagen, Studio City, Calif.) as described by the manufacturer. A second flask was transfected with 10 μg of empty pcDNA3 vector for use as a negative control. After 15 h of gene expression, the cells were washed with phosphate-free DME prior to labeling. The cells were then labeled by incubating each T-25 flask with 1.5 ml of phosphate-free DME supplemented with 10% dialyzed calf serum (Gibco/Invitrogen Corp.) and [^{32}P]orthophosphoric acid in water (1 mCi/T-25 flask) for 4 h at 37°C. Each flask was then washed twice with 1 ml of Hanks' balanced salt solution (Gibco/Invitrogen Corp.) prior to incubation in 80 μl of Triton lysis buffer (20 mM Tris-HCl [pH 7.5], 75 mM NaCl, 75 mM KCl, 20% glycerol, 4 mM $MgCl_2$, 1 mM DTT, 1 mM EDTA, 0.5% TX-100) containing 1× protease inhibitor mix and phosphatase inhibitors (1 mM Na_3VO_4, 25 mM β-glycerophosphate) for 15 min at 4°C. The cells were then removed from the flasks with a cell scraper, and insoluble materials were pelleted by centrifugation at $16,000 \times g$ for 1 min. The resulting supernatants were used for immunoprecipitation of NS5A as described below.

Inhibition of the mTOR/p70S6K pathway using rapamycin. COS-1 cells (0.5×10^6, in a T-25 flask) were transfected as described under "In vivo [^{32}P]orthophosphoric acid labeling." The cells were washed with phosphate-free DME and then incubated with or without 20 nM rapamycin. After 1 h at 37°C, the cells were labeled with phosphate-free DME supplemented with 10% dialyzed calf serum (Gibco/Invitrogen Corp.) and [^{32}P]orthophosphoric acid in water for 4 h. The cells were then processed as described under "In vivo [^{32}P]orthophosphoric acid labeling."

Immunoprecipitation of NS5A from cell lysates. Protein lysates prepared from 0.5×10^6 cells were incubated with 1 μg of anti-NS5A monoclonal antibody for 3 h at 4°C and then mixed with 50 μl of protein G-agarose beads (Boehringer Mannheim) for 2 h at 4°C (final volume, 1 ml). The beads were then washed three times with Triton lysis buffer containing 1× protease inhibitor mix and phosphatase inhibitors (1 mM Na_3VO_4, 25 mM β-glycerophosphate) prior to suspension in 50 μl of 2× SDS protein loading buffer (20% [vol/vol] glycerol, 4% [wt/vol] SDS, 0.125 M DTT). The immunoprecipitated NS5A was then resolved by SDS–10% PAGE and transferred to a nitrocellulose membrane, and the NS5A phosphorylation band was detected by autoradiography.

Immunoblot analysis of NS5A expressed in COS-1 cells. Immunoblot analysis was performed as previously described (28). Briefly, blots were probed with a monoclonal antibody against NS5A (4 μg/ml; ViroStat, Portland, Maine), followed by a 1:20,000 dilution of donkey anti-mouse immunoglobulin G conjugated to horseradish peroxidase (Jackson ImmunoResearch Laboratories, Inc., West Grove, Pa.). NS5A was then visualized by enhanced chemiluminescence (Amersham Biosciences Corp.).

RESULTS AND DISCUSSION

In vitro phosphorylation of NS5A by yeast protein kinases. Phosphorylation of NS5A is believed to affect its biological properties. However, NS5A lacks intrinsic protein kinase activity, suggesting that its phosphorylation results from interaction with one or more cellular kinases (10, 12–15, 25). Previous in vitro studies demonstrated that CK2 and cAMP-dependent protein kinase (PKA) are able to phosphorylate NS5A (12, 14). Since NS5A performs a host of diverse functions, including the modulation of several signal transduction pathways (6, 8, 28), we expect that NS5A may be phosphorylated by additional cellular kinases. To further investigate the phosphorylation of NS5A, we have taken advantage of GST-yeast kinase fusion proteins to screen the *S. cerevisiae* kinome for kinases that phosphorylate NS5A in vitro.

TABLE 1. Distribution by major groups of the GST-yeast kinases phosphorylating the HCV nonstructural protein NS5A[a]

Group	Kinase(s)
AGC	YMR104C, YDR466W
CMGC	YIL035C, YOR061W
CK1	YNL154C, YPL204W
STE	YPL140C
CaMK	YDL101C

[a] GST-protein kinase constructs representing 119 *S. cerevisiae* protein kinases were purified by glutathione-agarose chromatography and subjected to an in vitro kinase assay as described in Materials and Methods. Eight kinases were shown to phosphorylate NS5A and are listed in their respective group in this table. These kinases represent five major groups of yeast kinases: AGC (so named because this group includes protein kinases A, G and C), CMGC (so named because this group includes cyclin-dependent kinases, mitogen-activated protein kinase, glycogen synthase kinase 3, and casein kinase 2), CK1 (so named because this group includes casein kinase 1), STE (so named because this group includes STE7, a protein kinase of the MAPK kinase family), CaMK (so named because this group includes Ca^{2+}/calmodulin-dependent kinases). The groups are based in amino acid sequence homology of the known protein kinases. A regular yeast kinase assay is described in Fig. 1.

The yeast genome is predicted to contain 124 protein kinases, and 119 of these have been successfully expressed as GST-kinase fusion proteins (36). Eight of these constructs were capable of phosphorylating NS5A under the conditions described here. Table 1 provides a summary of the distribution by major groups of the GST-yeast kinases that phosphorylated NS5A in vitro, and autoradiographs from representative samples are presented in Fig. 1. In order to eliminate the possibility that phosphorylation would be influenced by the presence of a tag used to facilitate protein purification, we used native NS5A that was purified to homogeneity by sequential DEAE-Sepharose and Mono Q anion-exchange chromatography (13). hCK2, which phosphorylates NS5A in vitro (14), was used as a positive control to demonstrate NS5A phosphorylation (Fig. 1B, lanes 14 and 28).

The yeast kinases that phosphorylated NS5A did so with variable efficiencies. For example, comparison of lanes 2 and 3 demonstrates that the yeast kinase YPL204W (Fig. 1B, lane 3) generated a stronger ^{32}P signal associated with NS5A phosphorylation than did construct YNL154C (Fig. 1B, lane 2). This is not surprising, since these kinases are likely to have different affinities for NS5A and may also have different requirements for optimal activity. Because of the vast number of kinases screened in this study, the phosphorylation reactions were performed under identical conditions.

Several of the reactions revealed additional bands of phosphorylation that were presumably associated either with autophosphorylation of the kinase or with contaminants copurifying with the respective kinase. For example, although the YOL128C construct was unable to phosphorylate NS5A, a higher-molecular-weight band, presumably corresponding to the autophosphorylated kinase, was detected (Fig. 1, lane 16).

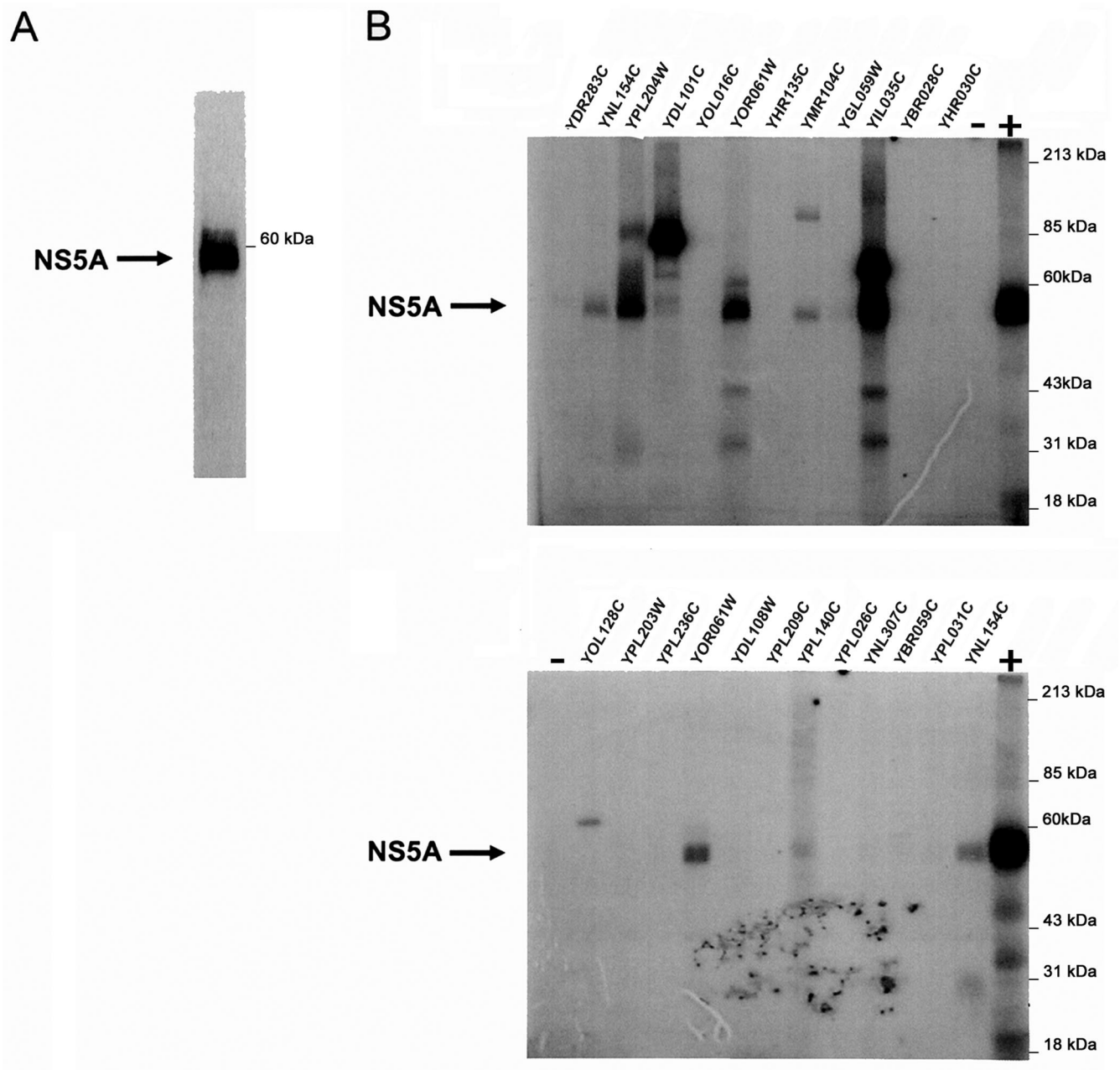

FIG. 1. Purity of the NS5A protein and in vitro phosphorylation of NS5A by yeast kinases. (A) The NS5A substrate used during this study was tested for its purity. Native recombinant NS5A (1 μg), purified from Sf9 cells, was resolved by SDS-PAGE and visualized by silver staining. The arrow indicates the NS5A protein. (This panel is reprinted with the permission of the publisher of reference 13 and is shown here to demonstrate the purity of the substrate, which was an essential prerequisite for our analyses.) (B) In a regular yeast kinase assay, baculovirus recombinant NS5A purified from Sf9 cells (100 ng) was phosphorylated in kinase buffer containing GST-yeast kinase bound to glutathione beads as described in Materials and Methods. The reaction was monitored by autoradiography of ^{32}P-labeled NS5A resolved by SDS-PAGE. Two autoradiography films from two regular yeast kinase assays are shown. The arrows show the NS5A protein. Human recombinant casein kinase 2 was used as a positive control to demonstrate phosphorylation of NS5A under the conditions described here. Yeast extracts from cells transfected with an empty glutathione vector were used as a negative control to demonstrate that phosphorylation of NS5A was not associated with proteins nonspecifically bound to either GST or the glutathione-agarose beads. The kinases present in the phosphorylation reaction were as follows: YDR283C (lane 1), YNL154C (lane 2), YPL204W (lane 3), YDL101C (lane 4), YOL016C (lane 5), YOR061W (lane 6), YHR135C (lane 7), YMR104C (lane 8), YGL059W (lane 9), YIL035C (lane 10), YBR028C (lane 11), YHR030C (lane 12), negative control (lane 13), positive control (lane 14), negative control (lane 15), YOL128C (lane 16), YPL203W (lane 17), YPL236C (lane 18), YOR061W (lane 19), YDL108W (lane 20), YPL209C (lane 21), YPL140C (lane 22), YPL026C (lane 23), YNL307C (lane 24), YBR059C (lane 25), YPL031C (lane 26), YNL154C (lane 27), and positive control (lane 28).

TABLE 2. Summary of the yeast kinases shown to phosphorylate NS5A and the related human kinases identified by sequence homology[a]

Yeast NS5A kinases		Kinase group	Related human kinases
ORF[b]	Name		
YPL204W	HRR25	CK1	CK1 delta isoform 1 (10^{-157}), CK1 delta isoform 2 (10^{-157}), CK1 epsilon (10^{-156}), CK1 alpha (10^{-149}), CK1 gamma1 (10^{-95})
YNL154C	YCK2	CK1	CK1 gamma 2 (7×10^{-95}), CK1 gamma 3 (5×10^{-93}), CK1 gamma 1 (5×10^{-92}), CK1 alpha (5×10^{-87}), CK1 delta (10^{-83})
YIL035C	CKA1	CMGC	CK2 (10^{-163}), GSK3 alpha (6×10^{-17}), GSK3 beta (6×10^{-16}), CDK-like 2 (9×10^{-14}), CDK-like 5 (10^{-13})
YOR061W	CKA2	CMGC	CK2 (10^{-138}), GSK3 beta (5×10^{-17}), GSK3 alpha (5×10^{-17}), CDK6 (4×10^{-12}), MAPK p38 beta (4×10^{-11})
YPL140C	MKK2	STE	MEK1 (4×10^{-50}), MEK2 (8×10^{-48}), MEK5 (8×10^{-42}), MKK7β (4×10^{-39}), MKK4 (4×10^{-39})
YDL101C	DUN1	CaMK	CHK2 (6×10^{-47}), Ca^{2+}/calmodulin-dependent kinase 1 (9×10^{-46}), double cortin-like and Ca^{2+}/calmodulin-dependent kinase-like 1 (5×10^{-45}), PKC mu (8×10^{-36}), PKD2 (8×10^{-35})
YMR104C	YPK2	AGC	SGK2 (3×10^{-96}), AKT3 (5×10^{-82}), p70S6K (4×10^{-79}), PKC theta (2×10^{-72}), p90S6K (10^{-71})
YDR466W	PKH1	AGC	AKT1 (10^{-65}), PDK1 (10^{-65}), p70S6K (3×10^{-22}), SGK1 (10^{-18}), PKA catalytic subunit beta (10^{-18})

[a] The yeast kinases shown to phosphorylate NS5A are summarized here, along with the major groups to which the kinases belong. Also included are the top five nonredundant hits resulting from database BLAST searches to identify related human protein kinases. These hits are sorted by the quality of the amino acid homology between the yeast kinases and the human kinases from best to worst, with the expected value (e-value) indicated in parentheses. The expected value is an estimate of the probability of a sequence occurring by random chance, given the BLAST database used for the search. A very low e-value indicates a good homology; a higher one indicates a poor homology. Some of the related human kinases shown here are highly conserved with the respective yeast kinase, while others are not. For example, the top five nonredundant hits to the yeast kinase YPL204C correspond to various CK1 species, all of which have high sequence homology (10^{-157} to 10^{-95}) with YPL204W. A similar situation is observed for YNL154C. By contrast, the top five nonredundant hits to the yeast kinases YIL035C and YOR061W represent candidates with a broader range of sequence homologies (10^{-163} to 4×10^{-11}). MAPK p38, PKC, PKA, PKD, and SGK stand, respectively, for mitogen-activated protein kinase p38, protein kinase C, cAMP-dependent protein kinase, protein kinase D, and serum/glucocorticoid-regulated kinase. The CK1, CMGC, STE, CaMK, and AGC abbreviations are explained in Table 1.

[b] ORF, open reading frame.

When the reaction was carried out in the presence of yeast extracts from cells transfected with an empty glutathione vector, no phosphorylation of NS5A was detected (Fig. 1, lanes 13 and 15). These results demonstrate that phosphorylation of NS5A is not associated with proteins nonspecifically bound to either GST or the glutathione-agarose beads. In addition, the yeast kinase GCN2, which has sequence homology with the interferon-inducible protein kinase PKR, did not phosphorylate NS5A (data not shown). This is consistent with our previous demonstrations that although NS5A can interact with PKR, it is not phosphorylated by this kinase (6).

Identification of human protein kinases related to yeast NS5A protein kinases. We used the sequences of the eight yeast kinases (http://www.ncbi.nlm.nih.gov/entrez/query.fcgi) that phosphorylated NS5A to perform a National Center for Biotechnology Information BLAST search (http://www.ncbi.nlm.nih.gov/BLAST) in order to identify human kinases with sequence homology. The human kinases identified by this approach included candidates from the CK1, CMGC, STE, CaMK, and AGC groups (Table 2). Consistent with previous studies demonstrating that CK2 (14) and PKA (12) phosphorylate NS5A, CK2 was identified as a top candidate for the CMGC group, represented by the yeast constructs YIL035C and YOR061W, and PKA was identified as a top candidate for the AGC group, represented by the yeast construct YDR466W. These observations support the validity of this approach and provided additional confidence that analysis of the human protein kinases present on this list would serve as a good starting point for subsequent in vitro NS5A phosphorylation studies. We therefore screened all the commercially available kinases corresponding to the top five nonredundant hits for each kinase group reported in Table 2, including CK2, MEK1, MKK7β1, CHK2, AKT1, p70S6K, SGK1, and PDK1. Because human kinase homologues were not available for CK1 delta and p90S6K, we screened the respective rat kinases.

In vitro phosphorylation of NS5A by human protein kinases. Consistent with previous studies (14), we found that hCK2 phosphorylated NS5A in vitro under the conditions described here (Fig. 2A, lane 3). Similarly, rCK1 delta also phosphorylated NS5A (Fig. 2A, lane 5). It should be noted that a faint lower-molecular-weight radiolabeled band was also detected in the phosphorylation reaction with hCK2. Since this band was also detected with hCK2 in the absence of NS5A in the kinase assay (Fig. 2A, lane 2), we suspect that this corresponds to phosphorylation of a contaminant present in the hCK2 preparation.

We also found that NS5A was phosphorylated by members of the STE group, including the mitogen-activated protein kinase kinase (MAPK kinase) family members hMEK1 (Fig. 3A, lane 4), hMKK6 (Fig. 3B, lane 4), and hMKK7β1 (Fig. 3C, lane 4). Although hMKK6 was not among the top five nonredundant hits, we chose to screen this kinase because it is nevertheless a closely related member of the MAPK family and was readily available. For each kinase tested, hCK2 was used as a positive control (Fig. 3A, B, and C, lanes 1). In each case, a second phosphorylated band was detected. Analysis of the kinases alone (Fig. 3A, B, and C, lanes 5) revealed that these bands were detected in the absence of NS5A, demonstrating that they are associated with the kinases. The observed molecular weights are consistent with those expected for each kinase, suggesting that these bands correlate to autophosphorylated kinases. This idea is supported by previous reports describing

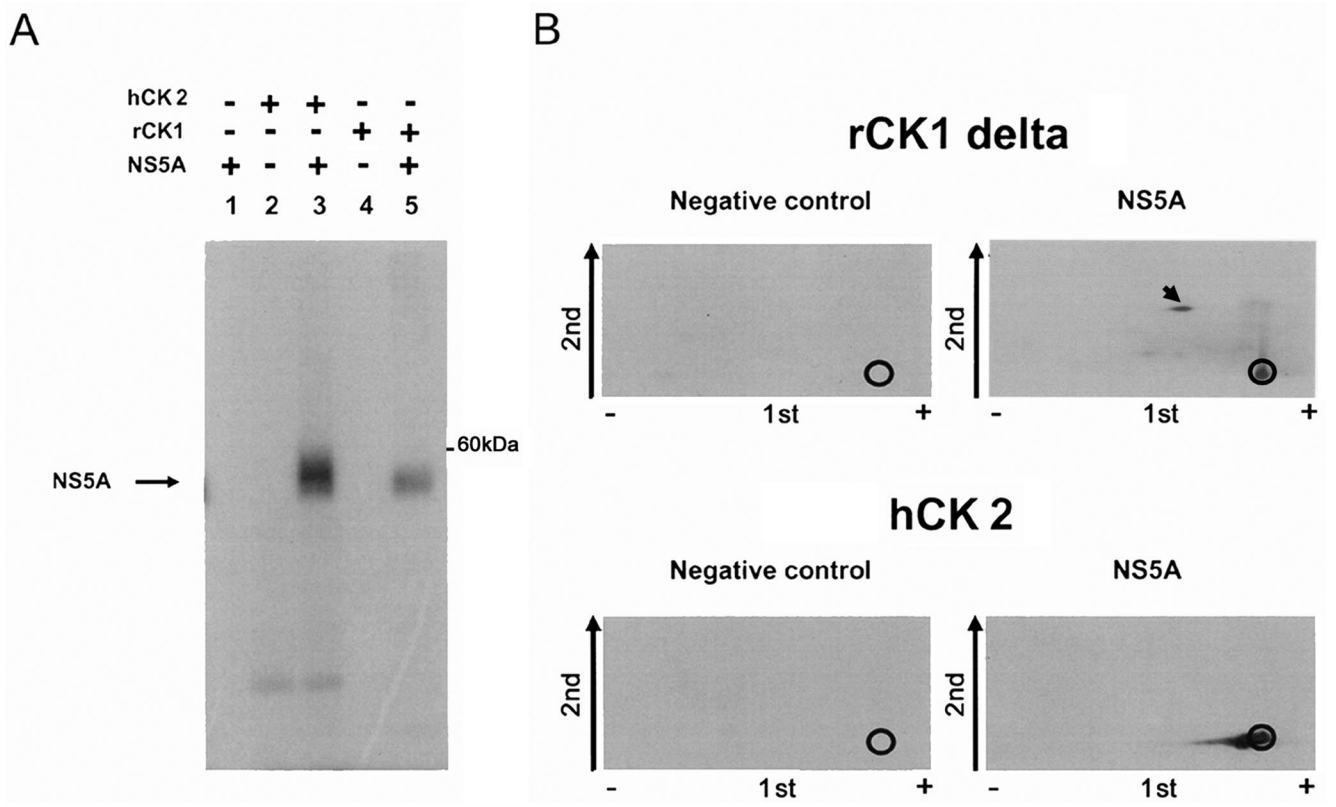

FIG. 2. In vitro phosphorylation of NS5A with CK1 delta and CK2. (A) Autoradiography of ^{32}P-labeled NS5A resolved by SDS-PAGE. The CK2 used in this experiment is a human kinase, and the CK1 delta is a rat kinase. The phosphorylation reactions carried out were as follows: NS5A minus kinase (lane 1), hCK2 minus NS5A (lane 2), hCK2 plus NS5A (lane 3), rCK1 minus NS5A (lane 4), and rCK1 plus NS5A (lane 5). (B) Phosphopeptide mapping of NS5A phosphorylated with either rCK1 or hCK2. In vitro-phosphorylated NS5A was resolved by SDS-PAGE, and the proteins were electroblotted onto nitrocellulose membranes. The radiolabeled NS5A bands were detected by autoradiography and subsequently sliced out and subjected to enzymatic digestion with trypsin and chymotrypsin. The peptides were applied on cellulose TLC plates at an origin shown by the black circle. The peptides were then separated in the first dimension by one-dimensional electrophoresis (1st). The positively charged peptides migrate toward the anode (negative plug [-]), and the negatively charged peptides migrate toward the cathode (the positive plug [+]). Using the same TLC plate, the peptides were resolved in the second dimension (shown by the arrow labeled 2nd) by ascending chromatography. The TLC plate was then exposed to film to generate the phosphopeptide map. The black dots show where the phosphopeptides are in the map. Phosphorylation reactions carried out in the absence of NS5A (shown in this panel) or in the presence of NS5A but not the kinase (not shown) were used as negative controls to test for peptides coming from potential contaminating proteins of molecular weight similar to that of NS5A or poorly resolved kinases. The NS5A map of the phosphorylation reaction carried out in the presence of NS5A but not the kinase gives an autoradiography without any signal (result not shown). The black arrow inside the CK1 panel shows the major NS5A peptide phosphorylated by CK1 delta.

the autophosphorylation of these kinases (2, 3). However, we cannot rule out the possibility that these bands represent contaminants in the kinase preparations.

Two of the top five candidates from the AGC kinase group, hAKT1 (Fig. 3D, lane 2) and hp70S6K (Fig. 3E, lane 2), phosphorylated NS5A in vitro. As was the case with kinases from the STE group, a second band of ^{32}P-labeled material that is likely to be an autophosphorylated form of the kinase was also detected (Fig. 3D and 3E, lanes 1) (26, 32). The remaining kinases from the AGC group (hPDK1, hSGK1, and rp90S6K) did not phosphorylate NS5A (data not shown), nor did hCHK2, the only commercially available kinase among the top five nonredundant hits of the CaMK group (Fig. 3F, lane 4). However, a member of the CaMK group not among the top five hits, Ca^{2+} calmodulin-dependent kinase II, was able to phosphorylate NS5A in vitro (data not shown). Although we did not independently verify whether the kinases that failed to phosphorylate NS5A were able to phosphorylate a known substrate, the presence of a signal associated with autophosphorylation suggests that these kinases were active.

In vitro phosphopeptide mapping of NS5A. The results described above demonstrated the utility of a high-throughput screen of the yeast kinome and revealed that human kinases from several major kinase groups were able to phosphorylate NS5A. In order to determine whether the sites of phosphorylation were unique for the different groups of kinases, we compared the phosphopeptide maps of in vitro-phosphorylated NS5A. Figure 2B shows the tryptic/chymotryptic phosphopeptide maps of NS5A phosphorylated with either rCK1 delta or hCK2. One labeled phosphopeptide detected in the presence of rCK1 delta, denoted by the arrow, was not detected with hCK2, suggesting that the phosphorylation sites may differ. Phosphopeptide maps generated with kinases from the STE kinase group (i.e., MAPK family member MEK1 or

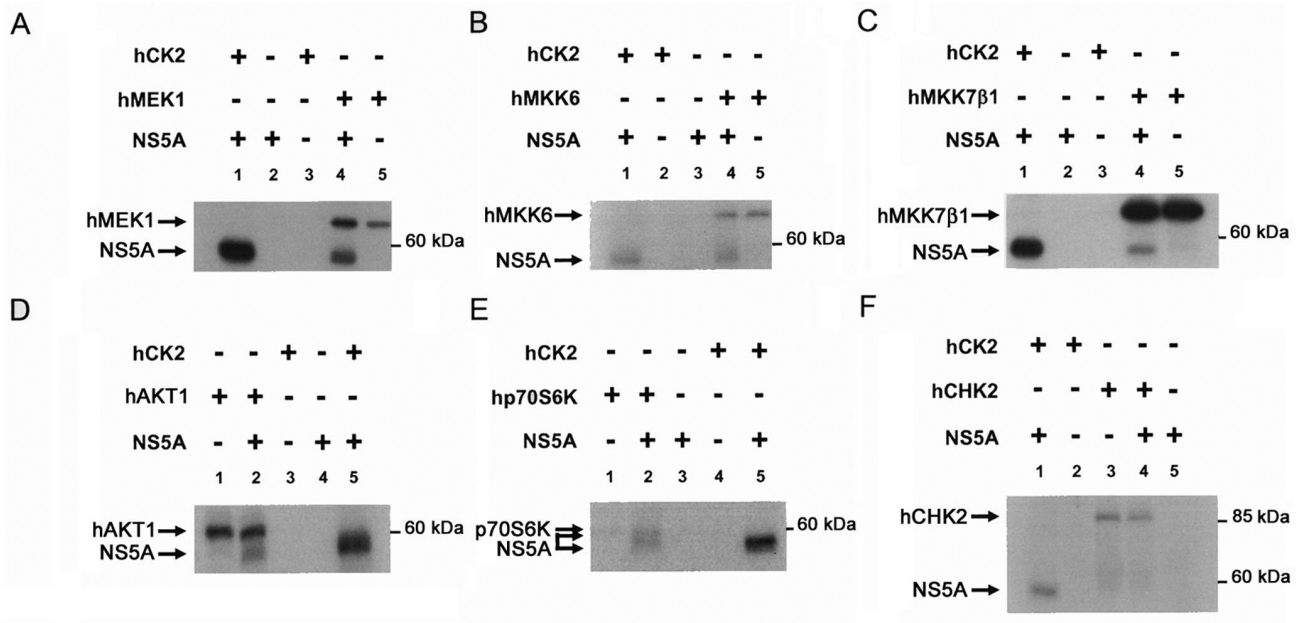

FIG. 3. In vitro phosphorylation of NS5A with members of the STE and AGC groups of human kinases. This figure shows the region of the autoradiography film around the molecular weight of NS5A incubated with or without different kinases. The kinase reactions were carried out with the related human kinases for the yeast kinases found to phosphorylate NS5A in this study. MEK1, MKK6, MKK7β1, AKT1, and p70S6K used in this study are human recombinant proteins. Baculovirus recombinant NS5A purified from Sf9 cells (100 ng) was phosphorylated in kinase buffer containing the appropriate human kinases as described under Materials and Methods. The reaction was monitored by autoradiography of ^{32}P-labeled NS5A resolved by SDS-PAGE. In each experiment, hCK2 was used as a positive control, demonstrating that NS5A was phosphorylated under the conditions used here. Arrows show NS5A or the kinase autophosphorylation. (A) Phosphorylation with hMEK1. Phosphorylation reactions carried out with NS5A in the presence of either hCK2 (lane 1) or hMEK1 (lane 4) are shown. Negative controls including incubation of NS5A (lane 2) or kinase alone (lanes 3 and 5) are shown for comparison. The arrows in this panel show two phosphoproteins, NS5A phosphorylated by hCK2 or hMEK1 and the autophosphorylation band of MEK1. (B) Phosphorylation with hMKK6. Phosphorylation reactions carried out with NS5A in the presence of either hCK2 (lane 1) or hMKK6 (lane 4) are shown. Negative controls including incubation of NS5A (lane 3) or kinase alone (lanes 2 and 5) are shown for comparison. The arrows in this panel show two phosphoproteins, NS5A phosphorylated by hCK2 or hMKK6 and the autophosphorylation band of MKK6. (C) Phosphorylation with hMKK7β1. Phosphorylation reactions carried out with NS5A in the presence of either hCK2 (lane 1) or hMKK7β1 (lane 4) are shown. Negative controls including incubation of NS5A (lane 2) or kinase alone (lanes 3 and 5) are shown for comparison. The arrows in this panel show two phosphoproteins, the NS5A phosphorylated by hCK2 or hMKK7β1 and the autophosphorylation band of hMKK7β1. (D) Phosphorylation with hAKT1. Phosphorylation reactions carried out with NS5A in the presence of either hCK2 (lane 5) or hAKT1 (lane 2) are shown. Negative controls including incubation of NS5A (lane 4) or kinase alone (lanes 1 and 3) are shown for comparison. The arrows in this panel show two phosphoproteins, NS5A phosphorylated by hCK2 or hAKT1 and the autophosphorylation band of hAKT1. (E) Phosphorylation with hp70S6K. Phosphorylation reactions carried out with NS5A in the presence of either hCK2 (lane 5) or hp70S6K (lane 2) are shown. Negative controls including incubation of NS5A (lane 3) or kinase alone (lanes 1 and 4) are shown for comparison. The arrows in this panel show three phosphoproteins, two bands for NS5A and one autophosphorylation band for hp70S6K. The phosphorylation of NS5A by hp70S6K produced two phosphopeptides. (F) Phosphorylation with hCHK2. Phosphorylation reactions carried out with NS5A in the presence of either hCK2 (lane 1) or hCHK2 (lane 4) are shown. Negative controls including incubation of NS5A (lane 5) or kinase alone (lanes 2 and 3) are shown for comparison.

MKK6) and the AGC kinase group (AKT1 and p70S6K) are shown in Fig. 4 and 5, respectively. The phosphopeptide patterns are quite distinct depending on the kinase used, demonstrating that NS5A can serve as a substrate for a variety of kinases, resulting in differential phosphorylation at multiple serine and threonine residues in vitro. Phosphopeptide maps were also generated from phosphorylation reactions carried out in the absence of NS5A in order to monitor for the presence of contaminating phosphopeptides (negative control). This was accomplished by cutting out and processing the same-molecular-weight region of the nitrocellulose membrane from lanes containing kinase only (see Materials and Methods). In some instances, we detected a significant amount of radiolabeled material in the absence of NS5A where no phosphopeptides were expected (i.e., negative control phosphopeptide maps with hAKT1 or hp70S6K) (Fig. 5). We suspect that this resulted from removal of some of the closely migrating kinase when the region of the filter corresponding to the molecular weight of NS5A was cut out for processing (see Fig. 3D and E, lanes 2). NS5A phosphopeptides detected in vitro that match with NS5A phosphopeptides detected in vivo are shown in Fig. 6 and discussed in more detail below.

In vivo phosphopeptide mapping of NS5A. In order to investigate the biological relevance of in vitro phosphorylation of NS5A by the kinases identified above, we next examined the phosphorylation of NS5A in cell culture. Briefly, COS-1 cells were transfected with a plasmid encoding the isogenic NS5A used for our in vitro studies, and in vivo-labeled NS5A was generated using [^{32}P]orthophosphate. Figure 6A shows an autoradiograph of NS5A immunoprecipitated with antibody specific to NS5A, resolved by SDS–10% PAGE, and transferred to a nitrocellulose membrane. Consistent with previous findings

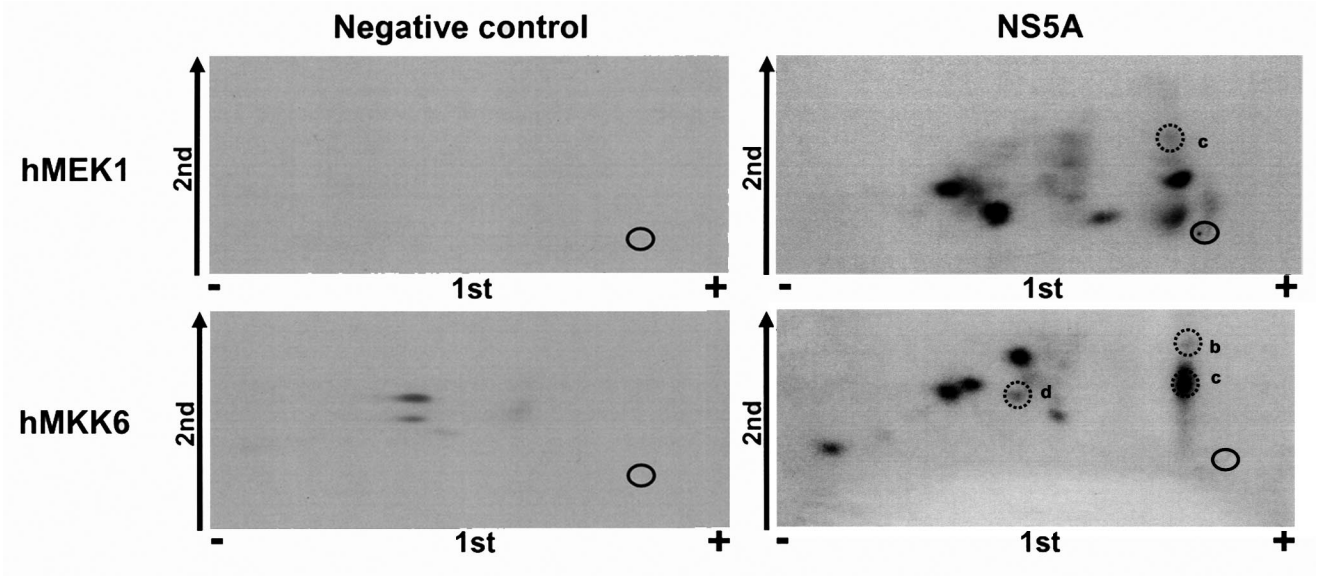

FIG. 4. Phosphopeptide mapping of NS5A phosphorylated in vitro with either hMEK1 or hMKK6. NS5A was phosphorylated with either the hMEK1 or hMKK6 kinase from the MAPK kinase family and subjected to phosphopeptide mapping as described in the legend to Fig. 3. The negative control panel is the analysis of the phosphopeptide signal from the phosphorylation reactions using hMEK1 or hMKK6 carried out in the absence of NS5A. The dotted circles labeled with letters are in vitro-labeled NS5A phosphopeptides that match with the NS5A phosphopeptides generated in vivo (see Fig. 6B).

(22, 30), two phosphorylated species of NS5A were detected. The identity of these bands was confirmed by immunoblot analysis with NS5A-specific monoclonal antibody (Fig. 6B). In addition, a third higher-molecular-weight species (150 kDa) was also detected during immunoprecipitation with cell lysates expressing NS5A (Fig. 6A, lane 1). We suspect that this may represent a binding partner of NS5A, since it was not detected in cell lysates transfected with a control vector lacking NS5A (Fig. 6A, lane 2). Each of the phosphorylated species of NS5A was subsequently processed for two-dimensional phosphopeptide mapping. Since the phosphopeptide maps generated from the two species of phosphorylated NS5A were nearly identical, Fig. 6C shows the tryptic/chymotryptic phosphopeptide map resulting from the lower-molecular-weight species. Immuno-

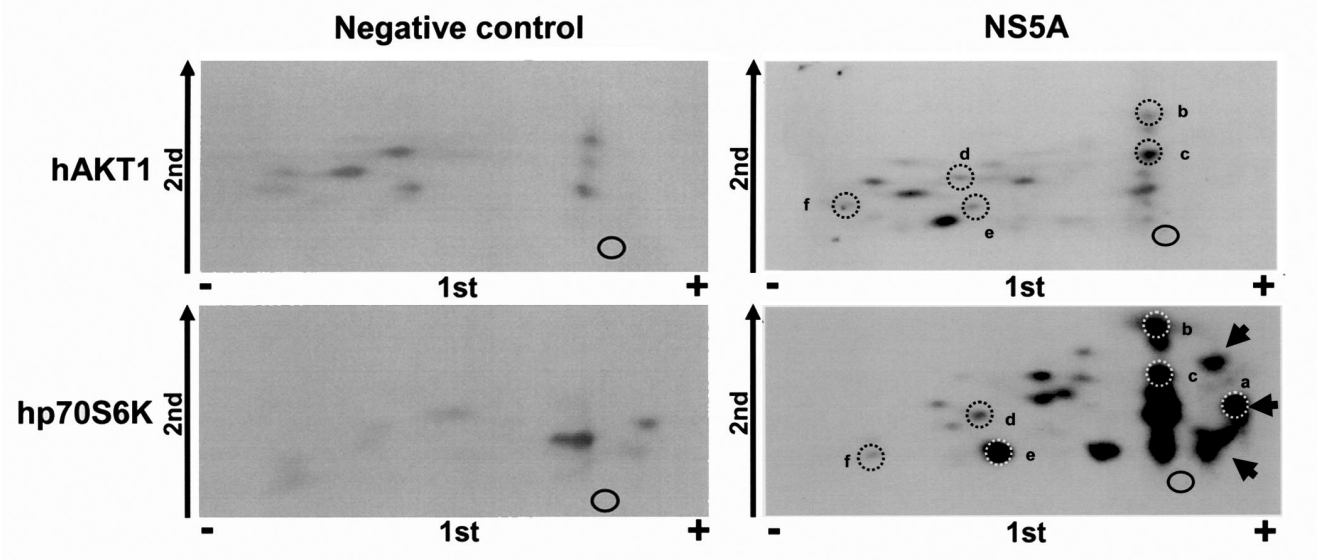

FIG. 5. Phosphopeptide mapping of NS5A phosphorylated in vitro with either hAKT1 or hp70S6K. NS5A was phosphorylated with either the hAKT1 or hp70S6K kinase and subjected to phosphopeptide mapping as described in the legend to Fig. 3. The negative control panel is the analysis of the phosphopeptide signal from the phosphorylation reactions using hAKT1 or hp70S6K carried out in the absence of NS5A. The three black arrows inside the phosphopeptide map of NS5A phosphorylated by hp70S6K show negatively charged NS5A phosphopeptides, which run toward the positive plug during the first dimension of the phosphopeptide map. The dotted circles labeled with letters are in vitro-labeled NS5A phosphopeptides that match the NS5A phosphopeptides generated in vivo (see Fig. 6B).

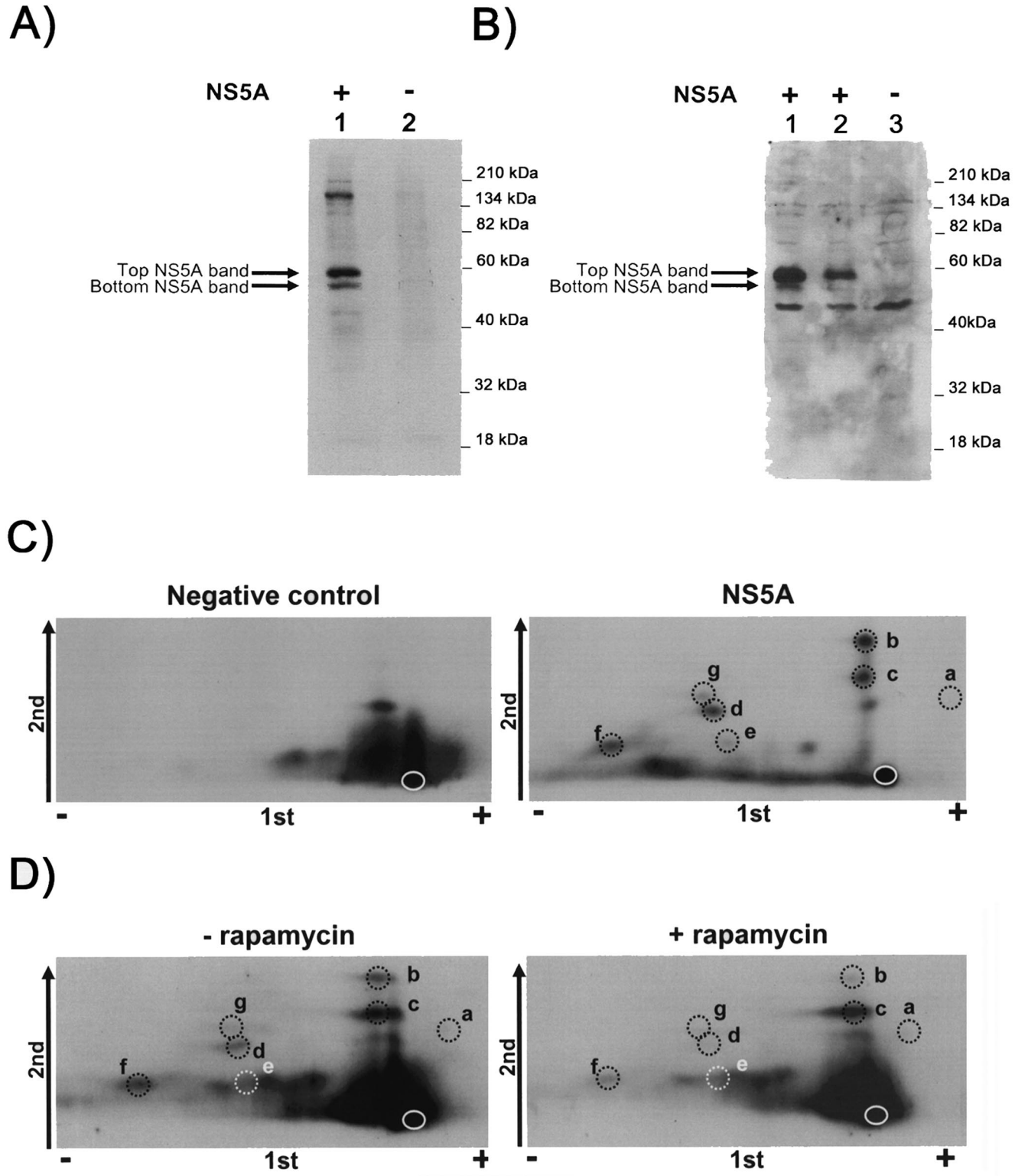

FIG. 6. Phosphopeptide mapping of NS5A phosphorylated in vivo. COS-1 cells were transiently transfected with 2 or 10 μg of plasmid encoding isogenic NS5A-1b used in this study for the in vitro NS5A maps. As a negative control, COS-1 cells were transfected with the empty plasmid vector. At 15 h posttransfection, cells were labeled with ^{32}P for 4 h at 37°C and harvested, and an antibody against NS5A was added for 3 h. The proteins associated with the NS5A antibody were isolated on protein G-agarose beads for 2 h at 4°C. The samples were immediately eluted with protein sample buffer, analyzed by SDS-PAGE (10% gel), and transferred to a nitrocellulose membrane. (A) An autoradiograph of the nitrocellulose membrane that contains the proteins isolated with the NS5A antibody and the protein G beads. (B) Immunoblot analysis of NS5A expressed in COS-1 cells. Nonradioactive cell lysates (200 ng) from cells transfected with 10 μg (lane 1), 2 μg (lane 2), or 0 μg (lane 3) of pcDNA3 NS5A-1b were resolved by SDS-PAGE (10% gel) and transferred to a nitrocellulose membrane prior to blotting with an NS5A-specific monoclonal antibody.

precipitates from protein lysates of COS-1 cells transfected with a control vector lacking NS5A were run in parallel, and the same-molecular-weight region of the nitrocellulose membrane was processed to monitor for the presence of contaminating phosphopeptides (Fig. 6C, negative control). Phosphopeptides unique to NS5A, as determined by comparison with the negative control, are labeled a to g.

The autoradiography films from the in vivo and in vitro phosphopeptide maps were then overlaid for comparison. The comigrating spots observed in the in vitro mapping experiments are given the same letter as for the in vivo map (compare Fig. 4 and 5 with Fig. 6). Interestingly, six of the seven phosphopeptides (labeled a to f) detected in vivo were also detected during in vitro phosphorylation of NS5A with hp70S6K (Fig. 5). Four of these phosphopeptides (labeled b, d, e, and f) were also detected when NS5A was phosphorylated with hAKT1 (Fig. 5). By contrast, only a small number of the peptides detected in vivo could also be seen during in vitro phosphorylation with either MEK1 or MKK6 (Fig. 4, phosphopeptide c for MEK1; phosphopeptides b, c, and d for MKK6).

One in vivo phosphopeptide (labeled g) was not detected in any of the in vitro phosphopeptide maps presented here. It is possible that this phosphopeptide resulted from the phosphorylation of NS5A by another kinase not characterized by two-dimensional phosphopeptide mapping in this study. Last, it is important to note that the in vivo phosphopeptide map reported here is more complex than what we previously observed (13). The conditions used here for enzymatic digestion of NS5A were more aggressive than those used in our previous study and more closely reflect those used to generate the distinct and complex phosphopeptide patterns reported for NS5A-1a (25). Therefore, we suspect that the increased complexity of the phosphopeptide maps observed for NS5A-1b is attributable to more complete enzymatic digestion.

Inhibition of the mTOR/p70S6K pathway using rapamycin. One of the most interesting and important kinases identified by our approach was p70S6K. It is well described in the literature that the mammalian target of rapamycin (mTOR) pathway is a major pathway activating p70S6K (21, 29, 33) and that rapamycin (21, 29, 33) is commonly used to study p70S6K activity. We therefore used rapamycin to investigate the in vivo contribution of p70S6K to the phosphorylation of NS5A. We already observed that on a one-dimensional SDS-PAGE gel, the phosphorylation of NS5A was significantly reduced by addition of rapamycin (data not shown), suggesting that the p70S6K activated by mTOR could play a role in the phosphorylation of NS5A. We then analyzed the phospho-NS5A-peptide map obtained from cells treated with or without rapamycin, and as shown in Fig. 6D, the phosphorylation of three of the major in vivo NS5A peptides phosphorylated by p70S6K (spots b, d, and f) was significantly reduced. However, as shown in Fig. 6D, rapamycin does not eliminate all the NS5A phosphopeptides (for example, spots a, c, and g), which suggests that this inhibitor is acting with specificity. This provides additional critical evidence that p70S6K and potentially closely related members phosphorylate NS5A in vivo.

Based on our findings, we suggest that hp70S6K is a human kinase responsible for phosphorylating NS5A in vivo. An examination of the sequence of the NS5A-1b species used here revealed sequences closely related to the consensus phosphorylation motifs of p70S6K (K/R-X-R-X-X-S/T-X). In addition, a slight variation in this motif is present around serine 2194, a highly conserved major phosphorylation site in NS5A-1b and in NS5A proteins from other HCV genotypes (13). In contrast, we were unable to detect this motif near serine 2321, a major phosphorylation site in the HCV 1a genotype (24). Further experiments using specific inhibitors or RNA interference (RNAi) strategies aimed at inhibiting or down-regulating the expression of the various kinases identified may provide further insight into the relative contributions of these kinases to the in vivo phosphorylation of NS5A.

Conclusions. It is likely that phosphorylation of NS5A plays a role in regulating the diverse functions of this protein. In this regard, we have been particularly interested in understanding the significance of NS5A phosphorylation in the ability of HCV to interfere with cellular signaling. For example, the interaction between NS5A and Grb2 may inhibit the MAPK pathway, resulting in down-regulation of cellular mRNA translation (22). In addition, NS5A plays a role in regulating viral mRNA translation initiation from the HCV internal ribosome entry site (9). Given the ability of NS5A to regulate mRNA translation, it is intriguing that NS5A was phosphorylated by both hAKT1 and hp70S6K, cellular kinases that themselves play important roles in translational control (1, 31, 34). Phosphorylation of NS5A by AKT and p70S6K could also induce HCV internal ribosome entry site-mediated translation, thereby facilitating HCV replication and persistence.

The two differentially phosphorylated species of NS5A are indicated by arrows. In addition, several nonspecifically reacting bands were detected, as evidenced by their presence in cell lysates in the presence or absence of transfection with pcDNA3 NS5A-1b. (C) In vivo phosphopeptide map of NS5A. Due to the clear resolution of the two NS5A bands, each band was analyzed individually. The autoradiograph of the map of the bottom NS5A band is shown here. As a negative control, the same-molecular-weight region of the immunoprecipitation from cells transfected with an empty plasmid was subjected to phosphopeptide mapping. Regular phosphopeptide mapping was done as described in Materials and Methods and in the legend to Fig. 3. The dotted circles show the specific in vivo NS5A phosphopeptides (labeled a to g). Each letter corresponds to a different phosphopeptide. This in vivo NS5A phosphopeptide autoradiograph was superimposed on each in vitro NS5A phosphopeptide map obtained in this study. The spots matching between the in vivo and in vitro maps have the same letters. (D) In vivo phosphopeptide map of NS5A expressed in COS-1 cells inhibited or not inhibited by rapamycin. This panel shows the phospho-NS5A-peptide map from cells inhibited or not inhibited with rapamycin. The autoradiograph of the map of the bottom NS5A band is shown here. The band from the same region of the immunoprecipitation from cells transfected with an empty plasmid and inhibited or not inhibited with rapamycin was subjected to phosphopeptide mapping and showed the same phosphopeptide pattern as the one seen in the negative control of panel C. The dotted circles show the localization of the phosphopeptides (labeled a to g) observed in the NS5A map in panel C. The ratios of the radioactivity counts between NS5A minus rapamycin and NS5A plus rapamycin for each phosphopeptide in the NS5A map in panel C have been calculated. These ratios are the following: a, 0.9; b, 5.0; c, 0.9; d, 11.5; e, 0.6; f, 4.4; g, 1.1. These ratios represent all experiments performed.

Clearly, the complexity of the in vivo phosphorylation patterns observed here warrants further experimentation to determine the significance of these findings. It is likely that multiple kinases, in addition to p70S6K, contribute to NS5A phosphorylation, including AKT, MEK1, and MKK6. In addition, although it is possible to positively identify kinases that phosphorylate NS5A in vivo, it is more difficult to rule out the possibility that other kinases may also contribute to NS5A phosphorylation. In this regard, it is also important that some of the kinases that phosphorylated NS5A in vitro may have no relevance in vivo and that in vitro assays may not detect biologically relevant NS5A kinases that require additional regulatory factors normally present in vivo. Nevertheless, our approach identified several kinases capable of phosphorylating NS5A. This information should facilitate the identification of the protein kinases that phosphorylate NS5A in liver cells, the natural site of HCV replication (7). Further studies aimed at evaluating the role of the identified NS5A kinases using in vivo model systems, such as the HCV replicon (18), may provide a better understanding of the role of NS5A phosphorylation during the HCV life cycle.

In summary, this study illustrates the use of a kinome-scale high-throughput screening approach for identifying protein kinases of interest. We propose that this approach represents an ideal model for other studies aimed at identifying protein kinases for further investigation of functionally relevant phosphorylation events. The development of similar approaches for characterizing gene function directly at the protein level should contribute significantly to the success of efforts in functional genomics, and such approaches may be generally applicable to the high-throughput purification and biochemical analysis of other proteins by mechanistic class.

ACKNOWLEDGMENTS

This work was supported by Public Health Service grant R01-AI47304 from the National Institute of Allergy and Infectious Diseases and grant P30DA015625 to the Center for Functional Genomics & HCV-Associated Liver Disease from the National Institute on Drug Abuse.

We thank Eric M. Phizicky at the University of Rochester, Rochester, N.Y., for providing us with the *S. cerevisiae* protein kinase constructs cloned in the plasmid pYEX4T-1 and expressed in the EJ758 yeast strain.

REFERENCES

1. **Chan, T. O., S. E. Rittenhouse, and P. N. Tsichlis.** 1999. AKT/PKB and other D3 phosphoinositide-regulated kinases: kinase activation by phosphoinositide-dependent phosphorylation. Annu. Rev. Biochem. **68:**965–1014.
2. **Deacon, K., and J. L. Blank.** 1997. Characterization of the mitogen-activated protein kinase kinase 4 (MKK4)/c-Jun NH2-terminal kinase 1 and MKK3/p38 pathways regulated by MEK kinases 2 and 3. MEK kinase 3 activates MKK3 but does not cause activation of p38 kinase in vivo. J. Biol. Chem. **272:**14489–14496.
3. **Deacon, K., and J. L. Blank.** 1999. MEK kinase 3 directly activates MKK6 and MKK7, specific activators of the p38 and c-Jun NH2-terminal kinases. J. Biol. Chem. **274:**16604–16610.
4. **Enomoto, N., I. Sakuma, Y. Asahina, M. Kurosaki, T. Murakami, C. Yamamoto, N. Izumi, F. Marumo, and C. Sato.** 1995. Comparison of full-length sequences of interferon-sensitive and resistant hepatitis C virus 1b. Sensitivity to interferon is conferred by amino acid substitutions in the NS5A region. J. Clin. Investig. **96:**224–230.
5. **Enomoto, N., I. Sakuma, Y. Asahina, M. Kurosaki, T. Murakami, C. Yamamoto, Y. Ogura, N. Izumi, F. Marumo, and C. Sato.** 1996. Mutations in the nonstructural protein 5A gene and response to interferon in patients with chronic hepatitis C virus 1b infection. N. Engl. J. Med. **334:**77–81.
6. **Gale, M., Jr., C. M. Blakely, B. Kwieciszewski, S. L. Tan, M. Dossett, N. M. Tang, M. J. Korth, S. J. Polyak, D. R. Gretch, and M. G. Katze.** 1998. Control of PKR protein kinase by hepatitis C virus nonstructural 5A protein: molecular mechanisms of kinase regulation. Mol. Cell. Biol. **18:**5208–5218.
7. **Gerber, M. A.** 1995. Pathobiologic effects of hepatitis C. J. Hepatol. **22:**83–86.
8. **He, Y., H. Nakao, S. L. Tan, S. J. Polyak, P. Neddermann, S. Vijaysri, B. L. Jacobs, and M. G. Katze.** 2002. Subversion of cell signaling pathways by hepatitis C virus nonstructural 5A protein via interaction with Grb2 and P85 phosphatidylinositol 3-kinase. J. Virol. **76:**9207–9217.
9. **He, Y., W. Yan, C. Coito, Y. Li, M. Gale, Jr., and M. G. Katze.** 2003. The regulation of hepatitis C virus (HCV) internal ribosome-entry site-mediated translation by HCV replicons and nonstructural proteins. J. Gen. Virol. **84:**535–543.
10. **Hirota, M., S. Satoh, S. Asabe, M. Kohara, K. Tsukiyama-Kohara, N. Kato, M. Hijikata, and K. Shimotohno.** 1999. Phosphorylation of nonstructural 5A protein of hepatitis C virus: HCV group-specific hyperphosphorylation. Virology **257:**130–137.
11. **Hunter, T., and G. D. Plowman.** 1997. The protein kinases of budding yeast: six score and more. Trends Biochem. Sci. **22:**18–22.
12. **Ide, Y., A. Tanimoto, Y. Sasaguri, and R. Padmanabhan.** 1997. Hepatitis C virus NS5A protein is phosphorylated in vitro by a stably bound protein kinase from HeLa cells and by cAMP-dependent protein kinase A-alpha catalytic subunit. Gene **201:**151–158.
13. **Katze, M. G., B. Kwieciszewski, D. R. Goodlett, C. M. Blakely, P. Neddermann, S. L. Tan, and R. Aebersold.** 2000. Ser(2194) is a highly conserved major phosphorylation site of the hepatitis C virus nonstructural protein NS5A. Virology **278:**501–513.
14. **Kim, J., D. Lee, and J. Choe.** 1999. Hepatitis C virus NS5A protein is phosphorylated by casein kinase II. Biochem. Biophys. Res. Commun. **257:**777–781.
15. **Koch, J. O., and R. Bartenschlager.** 1999. Modulation of hepatitis C virus NS5A hyperphosphorylation by nonstructural proteins NS3, NS4A, and NS4B. J. Virol. **73:**7138–7146.
16. **Lehman, C. W., D. S. King, and M. R. Botchan.** 1997. A papillomavirus E2 phosphorylation mutant exhibits normal transient replication and transcription but is defective in transformation and plasmid retention. J. Virol. **71:**3652–3665.
17. **Li, P., X. G. Gao, R. O. Arellano, and V. Renugopalakrishnan.** 2001. Glycosylated and phosphorylated proteins—expression in yeast and oocytes of Xenopus: prospects and challenges—relevance to expression of thermostable proteins. Protein Expr. Purif. **22:**369–380.
18. **Lohmann, V., F. Korner, J. Koch, U. Herian, L. Theilmann, and R. Bartenschlager.** 1999. Replication of subgenomic hepatitis C virus RNAs in a hepatoma cell line. Science **285:**110–113.
19. **Manning, G., D. B. Whyte, R. Martinez, T. Hunter, and S. Sudarsanam.** 2002. The protein kinase complement of the human genome. Science **298:**1912–1934.
20. **Martzen, M. R., S. M. McCraith, S. L. Spinelli, F. M. Torres, S. Fields, E. J. Grayhack, and E. M. Phizicky.** 1999. A biochemical genomics approach for identifying genes by the activity of their products. Science **286:**1153–1155.
21. **Mita, M. M., A. Mita, and E. K. Rowinsky.** 2003. Mammalian target of rapamycin: a new molecular target for breast cancer. Clin. Breast Cancer **4:**126–137.
22. **Neddermann, P., A. Clementi, and R. De Francesco.** 1999. Hyperphosphorylation of the hepatitis C virus NS5A protein requires an active NS3 protease, NS4A, NS4B, and NS5A encoded on the same polyprotein. J. Virol. **73:**9984–9991.
23. **Reed, K. E., A. E. Gorbalenya, and C. M. Rice.** 1998. The NS5A/NS5 proteins of viruses from three genera of the family *Flaviviridae* are phosphorylated by associated serine/threonine kinases. J. Virol. **72:**6199–6206.
24. **Reed, K. E., and C. M. Rice.** 1999. Identification of the major phosphorylation site of the hepatitis C virus H strain NS5A protein as serine 2321. J. Biol. Chem. **274:**28011–28018.
25. **Reed, K. E., J. Xu, and C. M. Rice.** 1997. Phosphorylation of the hepatitis C virus NS5A protein in vitro and in vivo: properties of the NS5A-associated kinase. J. Virol. **71:**7187–7197.
26. **Romanelli, A., V. C. Dreisbach, and J. Blenis.** 2002. Characterization of phosphatidylinositol 3-kinase-dependent phosphorylation of the hydrophobic motif site Thr(389) in p70 S6 kinase 1. J. Biol. Chem. **277:**40281–40289.
27. **Tan, S. L., and M. G. Katze.** 2001. How hepatitis C virus counteracts the interferon response: the jury is still out on NS5A. Virology **284:**1–12.
28. **Tan, S. L., H. Nakao, Y. He, S. Vijaysri, P. Neddermann, B. L. Jacobs, B. J. Mayer, and M. G. Katze.** 1999. NS5A, a nonstructural protein of hepatitis C virus, binds growth factor receptor-bound protein 2 adaptor protein in a Src homology 3 domain/ligand-dependent manner and perturbs mitogenic signaling. Proc. Natl. Acad. Sci. USA **96:**5533–5538.
29. **Tang, S. J., G. Reis, H. Kang, A. C. Gingras, N. Sonenberg, and E. M. Schuman.** 2002. A rapamycin-sensitive signaling pathway contributes to long-term synaptic plasticity in the hippocampus. Proc. Natl. Acad. Sci. USA **99:**467–472.
30. **Tanji, Y., T. Kaneko, S. Satoh, and K. Shimotohno.** 1995. Phosphorylation of hepatitis C virus-encoded nonstructural protein NS5A. J. Virol. **69:**3980–3986.

31. **Thomas, G., and M. N. Hall.** 1997. TOR signalling and control of cell growth. Curr. Opin. Cell Biol. **9:**782–787.
32. **Toker, A., and A. C. Newton.** 2000. Akt/protein kinase B is regulated by autophosphorylation at the hypothetical PDK-2 site. J. Biol. Chem. **275:** 8271–8274.
33. **von Manteuffel, S. R., A. C. Gingras, X. F. Ming, N. Sonenberg, and G. Thomas.** 1996. 4E-BP1 phosphorylation is mediated by the FRAP-p70s6k pathway and is independent of mitogen-activated protein kinase. Proc. Natl. Acad. Sci. USA **93:**4076–4080.
34. **Wang, X., F. E. Paulin, L. E. Campbell, E. Gomez, K. O'Brien, N. Morrice, and C. G. Proud.** 2001. Eukaryotic initiation factor 2B: identification of multiple phosphorylation sites in the epsilon-subunit and their functions in vivo. EMBO J. **20:**4349–4359.
35. **Zhou, Y., and L. Ratner.** 2000. Phosphorylation of human immunodeficiency virus type 1 Vpr regulates cell cycle arrest. J. Virol. **74:**6520–6527.
36. **Zhu, H., J. F. Klemic, S. Chang, P. Bertone, A. Casamayor, K. G. Klemic, D. Smith, M. Gerstein, M. A. Reed, and M. Snyder.** 2000. Analysis of yeast protein kinases using protein chips. Nat. Genet. **26:**283–289.